Analyst

Protective Mechanism of Dried Blood Spheroids: Stabilization of Labile Analytes in Whole Blood, Plasma, and Serum

Journal:	*Analyst*
Manuscript ID	AN-ART-06-2021-001132.R1
Article Type:	Paper
Date Submitted by the Author:	16-Sep-2021
Complete List of Authors:	Frey, Benjamin; The Ohio State University, Chemistry and Biochemistry Damon, Deidre; Ohio State University, Chemistry and Biochemistry Allen, Danyelle; Ohio State University, Chemistry and Biochemistry Baker, Jill; Ohio State University, Chemistry and Biochemistry Badu-Tawiah, Abraham; The Ohio State University, Chemistry and Biochemistry Asamoah, Samuel O; Ohio State University

ARTICLE

Protective Mechanism of Dried Blood Spheroids: Stabilization of Labile Analytes in Whole Blood, Plasma, and Serum

Received 00th January 20xx,
Accepted 00th January 20xx

DOI: 10.1039/x0xx00000x

Benjamin S. Frey,[a] Deidre E. Damon,[a] Danyelle M. Allen,[a] Jill Baker,[a] Samuel Asamoah[a] and Abraham K. Badu-Tawiah*[a]

Three-dimensional (3D) dried blood spheroids form when whole blood is deposited onto hydrophobic paper and allowed to dry in ambient air. The adsorbed 3D dried blood spheroid present at the surface of the hydrophobic paper is observed to offer enhanced stability for labile analytes that would otherwise degrade if stored in the traditional two-dimensional (2D) dried blood spot method. The protective mechanism for the dried blood spheroid microsampling platform was studied using scanning electron microscopy (SEM), which revealed the presence of a passivation thin film at the surface of the spheroid that serves to stabilize the interior of the spheroid against environmental stressors. Through time-course experiments based on sequential SEM analyses, we discovered that the surface protective thin film forms through the self-assembly of red blood cells following the evaporation of water from the blood sample. The bridging mechanism of red blood cell aggregation is evident in our experiments, which leads to the distinct rouleau conformation of stacked red blood cells in less than 60 min after creating the blood spheroid. The stack of self-assembled red blood cells at the exterior of the spheroid subsequently lyse to afford the surface protective layer detected to be approximately 30 μm in thickness after three weeks of storage in ambient air. We applied this mechanistic insight to plasma and serum to enhance stability when stored under ambient conditions. In addition to physical characterization of these thin biofilms, we also used paper spray mass spectrometry (MS) to examine chemical changes that occur in the stored biofluid. For example, we present stability data for cocaine spiked in whole blood, plasma, and serum when stored under ambient conditions on hydrophilic and hydrophobic paper substrates.

Introduction

The collection of biofluid microsamples has become increasingly important for clinical applications,[1,2] disease diagnostics,[3,4] and basic research.[5,6] These microsamples are conventionally collected via stick of extremities by lancet or by swabbing. As such, these sampling methods are non-invasive when compared to intravenous collection of larger samples. There is an increased demand for room-temperature storage of biofluid samples during transportation or when extended storage time is required, especially in resource-limited settings.[7] These have encouraged the development of methods and technology to stabilize biofluids stored at room temperature. Biopreservation of samples is necessary when there is a delay in sample processing or when expedited temperature-controlled delivery is unavailable to reduce degradation of analyte molecules prior to analysis.

Stabilization of biofluid samples at room temperature can be achieved by inducing changes in the intra- and intermolecular interactions that occur in the chemical microenvironment. Enhanced stability of targeted analytes in blood spot samples has been demonstrated through rapid heating, use of mesoporous silica nanoparticles, and chemical additives such as sodium fluoride,3-deazaadenosine, and silk-based proteins.[8–13] While these methods show promise in their ability to stabilize whole blood samples, their applications are limited to specific conditions, only stabilizing specific molecules for a moderately increased timeframe. Almost all these methods induce rapid cellular hemolysis upon drying in ambient air. Historically, dried blood spots (DBS) have been used as a popular platform for blood microsampling and storage due to ease of transport, simplicity, and cost effectiveness. Although the DBS methodology shows increased stability of some molecules, environmental stress due to the presence of moisture (humidity),[14,15] light,[16] and heat have been shown to deteriorate samples prior to analysis, giving rise to false negative results due to loss in sample integrity.[17–19]

To improve upon the DBS microsampling method, we recently described a dried blood spheroid platform that utilizes chemically modified hydrophobic paper (Figure 1A).[20] The main difference between the two paper-based microsampling methods is that DBS collect blood through an absorption mechanism whereas the dried blood spheroid platform works via an adsorption process (Figure 1B and C). Aqueous-based samples (e.g., blood, plasma, and serum) applied on hydrophobic paper beads up on the surface due to the marked

[a]*Department of Chemistry and Biochemistry, The Ohio State University, Columbus OH 43210.*
*Email: badu-tawiah.1@osu.edu
Electronic Supplementary Information (ESI) available: see DOI: 10.1039/x0xx00000xxx00000x

difference between the surface tension (γ) of the sample (e.g., γwater = 72 mN/m) and the surface energy of the hydrophobic paper substrate (~47.3-49.39 mN/m).[21] For viscous samples such as blood, the spherical shape of the drop initially present at the surface of the hydrophobic paper slowly forms a hemispheroid upon drying, yielding what we referred to as a dried blood spheroid (Figure 1C).

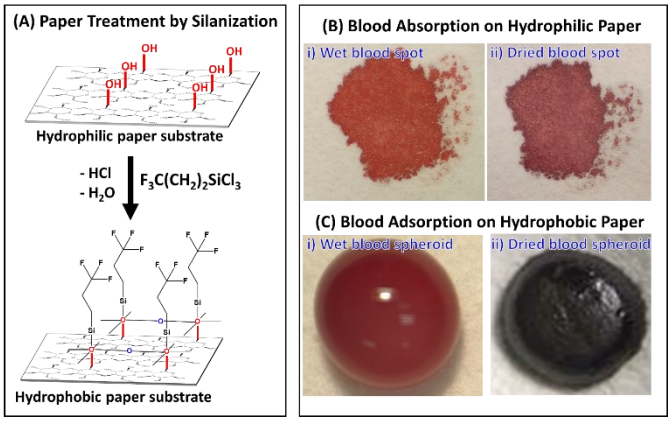

Figure 1. (A) Self-assembly chemistry for creating hydrophobic paper using gas-phase trichloro(3,3,3-trifluoropropyl)silane reagent. (B) Photographs of whole blood samples prepared using the conventional dried blood spot microsampling method that collect samples through an absorption process for wet blood (Bi) and dried blood (Bii) spots on the hydrophilic paper. (C) Photographs showing whole blood deposited on hydrophobic paper substrate as (Ci) wet blood and (Cii) dried blood spheroids via an adsorption mechanism. We used 10 µL of whole blood for both microsampling methods on hydrophobic paper substrates treated for 30 min with trichloro(3,3,3-trifluoropropyl)silane.

In the initial work, we speculated that due to the three-dimensional (3D) nature of the dried blood spheroid, the interior of the spheroid would be protected through the mechanism of critical radius of insulation. That is, the reduced surface area-to-volume ratio of the spheroid (compared with DBS) should limit the exposure of the interior to oxidative stress, which leads to the stabilization of labile analytes stored in dry blood at room temperature. Indeed, we have observed improved stability of enzymes and labile small organic compounds (e.g., diazepam and cocaine) under the dried blood spheroid storage conditions compared with the typical DBS method.[20] Aside from prolonged analyte stabilization under ambient conditions without cold storage, other notable advantages associated with adsorption of biofluids as spheroids include 1) the capacity to use small sample volumes due to the fact that reduced sample-paper interactions enables dramatic improvement in the recovery of small organic molecules, and 2) important secondary phenomena such as chromatographic and hematocrit effects that often lead to irreproducible analyte quantification from DBS are eliminated when using hydrophobic paper for blood collection due to the complete exclusion of biofluid diffusion.[20–22]

In the present study, we focused on investigating the physical changes that occur in the dried blood spheroid during the initial stages of drying to fully understand the mechanism governing analyte stabilization. Two novel aspects are presented: (1) new mechanistic insight for the protective properties of dried blood spheroids derived from scanning electron microscopy (SEM) and (2) enhanced stability of labile molecules in dried plasma and serum samples stored under room temperature conditions, which were examined by paper spray mass spectrometry (MS). We report the first experimental evidence for the bridging mechanism of red blood cell aggregation in these 3D blood spheroids on hydrophobic paper substrate, which is an important supplement to the widely accepted depletion mechanism. We also present stability data for cocaine in plasma and serum. The sol-gel transition of proteinaceous molecules in plasma and serum is likely the main contributing factor for providing enhanced stability to labile analytes contained within the interior bulk of these biofilms.[23]

Experimental Section

Chemicals and Reagents

Standard solutions of cocaine (1.0 mg/mL) and cocaine-d3 (100 µg/mL) were obtained from Cerilliant (Round Rock, TX). All solvents (Methanol (99.9%, HPLC grade), Ethyl Acetate (≥ 99.5 %), Acetonitrile (HPLC plus grade)), Glutaraldehyde solution (Grade 1, 25% in water), Trichloro(3,3,3-trifluoropropyl)silane (97%) were obtained from Sigma-Aldrich (St. Louis, MO). 18.2 MΩ water was obtained from a Milli-Q water purification system (Millipore, Billerica, MA, USA). Human blood from a healthy single donor was collected in K2 EDTA-capped blood collection tubes and lithium heparin collection tubes from Medline (Northfield, IL) with IRB exemption. All experiments were performed in accordance with the guidelines of the Office of Responsible Research Practices (ORRP) and approved by the ethics committee at The Ohio State University. Informed consents were obtained from human participants of this study. Human plasma and serum were isolated from whole blood in lab via centrifugation. 1X Phosphate Buffered Saline Tablets and phosphate buffer solution (1.0 M, pH 7.4) were purchased from AMRESCO (Solon, Ohio). Whatman chromatography filter paper (grade 1) was purchased from Whatman (Little Chalfont, England).

Paper Spray (PS) Mass Spectrometry

Mass spectra were recorded using Thermo Scientific Velos Pro LTQ linear ion trap mass spectrometer (San Jose, CA). MS parameters used were as follows: 200 °C capillary temperature, three microscans, and 60% Slens voltage. Spray voltage was 5 kV unless otherwise specified. The paper triangles were held in line with the inlet at a tip-to-inlet distance of 5 mm. Thermo Fisher Scientific Xcalibur 2.2 SP1 software was applied for MS data collecting and processing. Tandem MS with collision-induced dissociation (CID) was utilized for analyte identification. For the CID tests, 1.0 Th (mass/charge units) for the isolation window and 22-43 (manufacturer's unit) of normalized collision energy were chosen.

Scanning Electron Microscopy (SEM)

Dried biofluid samples (blood, plasma, serum) on paper squares were fixed in 2.5% glutaraldehyde in 0.1 M phosphate buffer pH 7.4 for a minimum of 72 hours. Samples were then rinsed 2 × 5 minutes with 1XPBS and then 2 × 5 minutes in water. Samples were then allowed to dry overnight in ambient air and sputter coated with a thin layer of AuPd or Au. The samples analyzed for thin film thickness were analyzed without any metal coating at room temperature with a water vapor pressure of 50 Pa in the chamber. A FEI Nova 400 NanoSEM, FEI Quanta 200 SEM and Thermo Scientific Apreo LoVac Analytical SEM were used to collect images. ImageJ software was utilized to measure thin film thickness.

Results and discussion

Overall Experimental Design/Procedure

The overall workflow of our experiments is illustrated in Figure 2 where we used paper spray (PS) MS to evaluate chemical changes in the form of analyte stability and SEM to examine physical microscopic morphological changes in the spheroids.

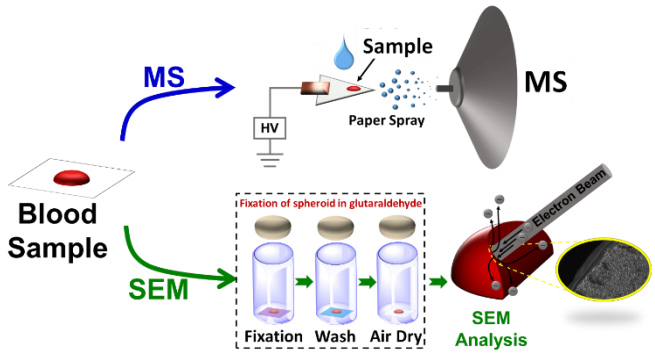

Figure 2. Analytical experimental workflow involving direct analysis of dry blood by PS MS (top sequence) and scanning electron microscopy analysis following sample fixation with glutaraldehyde (bottom sequence). Blood samples were fixed at different stages of the spheroid drying process to create various snapshots of the condition of red blood cells.

SEM analysis (Figure 2, bottom sequence) revealed a passivation thin film at the superficial surface of the spheroid, which is mainly responsible for protecting the interior of the spheroid. We applied this insight to stabilize labile organic compounds in dried plasma and serum samples. Although plasma and serum lack red blood cells (RBC), they contain several other large biomacromolecules that can undergo self-assembly processes. For example, sol-gel transitions have been shown to occur in plasma samples deposited onto glass microscope slides, leading to thin film formation which yield characteristic pattern formations that may be used in disease diagnosis.[24,25] SEM imaging of plasma and serum samples deposited on hydrophobic paper show that 3D thin biofilms form upon drying (Figures S1-S4). No observable passivation surface thin film was noted when compared to whole blood samples, suggesting that clotting factors and other proteins contribute to forming a protective layer in these biofluids. Conventional dried plasma spots (DPS) and dried serum spots (DSS) are found to be very unstable when stored at room temperature. The formation of 3D thin biofilms (e.g., plasma and serum) on hydrophobic paper enables enhanced stability compared with the 2D nature of DPS and DSS.

As stated above, paper substrate was chosen for the dried blood spheroid platform due to its wide availability and low-cost. Such properties make implementation in resource-limited settings easier. Another advantage associated with the use of paper substrate is that it enables direct analysis of the dried blood spheroid samples via PS MS (Figure 2, upper sequence). In this substrate-based ambient ionization method, complex sample (e.g., dried blood, plasma, or serum) present on a paper triangle is ionized simply by applying a suitable solvent (e.g., ethyl acetate) to selectively extract analytes from the sample followed by the application of direct current (DC) high voltage (3-5 kV), which initiates the generation of charged droplets from the extract. The resulting charged droplets ionize the analyte during transfer to the proximal mass spectrometer. Recent developments have shown that modified paper substrates (e.g., metal oxide deposition,[26] metal organic framework coated,[27] carbon nanotube coated,[28] silica coated[29]) provide enhanced PS performance compared with the unmodified paper substrate. Therefore, the use of hydrophobic paper for sample collection not only provides stability for labile compounds but also has created an avenue by which analytes present in the biofluid can be detected by MS with high sensitivity and accuracy via hydrophobic substrate spray ionization.[21,22,30,31] Another notable advantage for using hydrophobic paper over hydrophobic polymeric membranes is related to the cellulose core in the hydrophobic paper, which is found to be more friendly towards organic spray solvents that are necessary for the extraction of organic compounds from aqueous-based biofluids. Most synthetic hydrophobic membranes buckle when exposed to organic solvents yielding unstable signal when employed in substrate spray ionization.

Physical Characterization of Dried Blood

3D dried blood spheroid and 2D DBS samples were prepared on hydrophobic and hydrophilic paper substrates, respectively, and subsequently characterized by SEM after fixation with 2.5% glutaraldehyde in 0.1 M phosphate buffer (pH 7.4) for a minimum of 72 hours. Rapid hemolysis (i.e., the lysis of red blood cells) was observed in DBS samples in which no intact RBCs were detected after 2 h of drying the samples under ambient conditions (Figure S5). This result is consistent with previous reports which asserts that hemolysis in 2D blood films can be limited only after the sample is enclosed in an air-tight container, which is in turn stored at cold temperatures.[32,33] Not surprisingly, several studies have shown that the rapid hemolysis in DBS is accompanied by the degradation of labile compounds. On the contrary, SEM analysis of 3D dried blood spheroids revealed a different hemolysis pattern (Figure S6).

The typical drying time for 10 µL blood spheroid is approximately 2 h compared with 20 min for DBS. The SEM images for spheroids dried for 1 h are shown in Figures 3A and C for the exterior and interior surfaces of the 10 µL dried blood spheroids, respectively. The slow evaporation of water from the blood spheroid leads to self-assembly of intact RBCs. Only the RBCs at the surface of the dried blood spheroid were observed to lyse (Figure 3B and S6B, S6C and S6D), which led to the formation of a passivation layer of thin film that protects the interior of the spheroid. For example, a surface layer of about 30 µm thickness (Figure 3E) was observed after of spheroid was stored under ambient conditions for 21 days. The protective power of the surface thin film was revealed when the interior of the 21-day spheroid was also imaged, showing the presence of intact RBCs (Figure 3D). Although the RBCs are dehydrated, the dried blood spheroid methodology represents the first dry-state microsampling platform that has the capacity to stabilize RBCs without cold storage for an extended period of time. Such a low-cost, paper-based blood collection platform capable of limiting hemolysis in the dry state at room temperature has the potential to expand the current scope of application of the traditional DBS method by enabling diagnosis of diseases (e.g., malaria, anemia, and polycythemia) that are related to RBCs to be performed in resource-limited settings. That is, this technique effectively allows for on-site sample collection away from the clinic, enabling both symptomatic and asymptomatic patients to be reached for monitoring and proper administration of treatment.

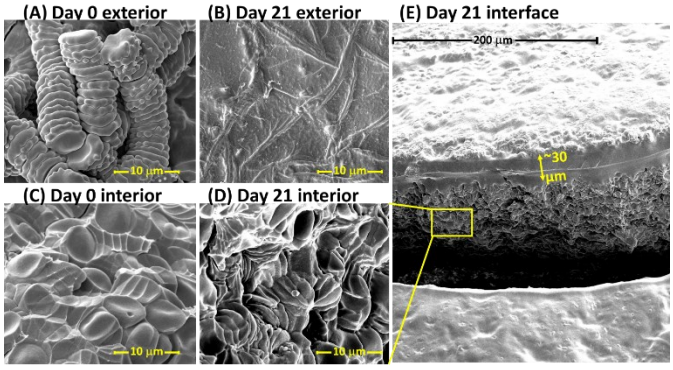

Figure 3. Scanning electron micrograph of the exterior (A, B) and interior (C, D) of a 10 µL dried blood spheroid, with a micrograph of a large interfacial area shown in E. (A) Exterior surface of a 10 µL dried blood spheroid after drying under ambient storage conditions for 1 h. The rouleau conformation of stacked red blood cells are observed at the spheroids surface after drying the blood for 1 h. (B) Exterior surface of a 10 µL dried blood spheroid after drying under ambient storage conditions for 21 days. No distinct red blood cells are detected. (C) Interior surface of a 10 µL dried blood spheroid after drying under ambient storage conditions for 1 h. Red blood cells persist in clusters and stacks of rouleau; distinct red blood cells are observable. (D) Interior of 10 µL dried blood spheroid after drying under ambient storage conditions for 21 days, zoomed-in from the interfacial photo in E. Red blood cells are still distinguishable and exist in clusters, including stacks of rouleau. (E) Interface showing exterior and interior of a 21-day-old dried blood spheroid. A distinct thin barrier approximately 30 µm of lysed red blood cells is observed that is believed to protect the interior of the dried spheroid.

Initial evidence for the protective power of the surface thin film was garnered in our previous study in which a much faster rate of decay was observed for dry diazepam samples derived from solutions prepared from pure water compared with when the diazepam analyte was spiked into whole blood.[20] We speculated that the rapid rate of decay observed for neat water samples was due to the absence of biomacromolecules, resulting in the formation of a 2D disk of dry diazepam on the hydrophobic paper substrate that increased exposure to oxidative stress. In contrast, whole blood is a colloidal mixture comprised of several large biomacromolecular components such as RBCs. We monitored the spheroid drying process by analyzing the exterior of the resulting dried blood spheroid with SEM to investigate how the RBCs self-assemble. The onset of RBCs aggregation was detected as early as 30 min after the drying process has begun (Figure S7A and S7D), where individual RBCs connected by tiny bridging films were observed. RBCs are thought to aggregate when 1) brought in close proximity due to the interaction with larger proteins or polymer (bridging mechanism) or 2) the concentration of protein or polymer at a surface is less than the suspending medium, causing osmotic flow away from the edges, leading to attractive forces (depletion mechanism).[34] SEM imaging of the drying of spheroids is consistent with the bridging model of RBC aggregation where proteins/polymers (e.g., fibrinogen) are thought to bridge two adjacent cells causing them to aggregate when the bridging force exceeds repulsive electrostatic forces.[35,36] There is additional evidence that the depletion mechanism occurs due to a concentration gradient of protein/polymers at the cellular surface, thereby creating attractive forces that drives aggregation of RBCs.[35,37] It is important is note that at this point (30 min) in the spheroid drying process, the RBCs are randomly orientated relative to each other with an average distance of 6.0 ± 0.4 µm (n = 19 RBCs). The RBCs are observed to closely pack together in an orderly manner to form the well-known rouleau conformation (i.e., linear arrays of stuck RBCs, Figure 3A) when drying time was increased to 1 h (see also Figure S7B, S7E). The 10 µL blood spheroid does not completely dry until after 120 min (Figure S7C, S7F). Therefore, we collected more SEM images (at 80- and 100-min drying times) to investigate how the rouleau conformation transitions from the regular array of distinct RBCs to the large conglomerate that constitutes the protective surface film. These experiments revealed that the RBCs residing at the exterior of the spheroid (i.e., blood-air interface) begin to lose their disc-like shape at approximately 80 min after formation in ambient air (Figure S8A). Compared with 100 min drying time (Figure S8B), more remnants of the rouleau conformation were observed at 80 min drying time as well as spiny RBCs that are undergoing dehydration and hemolysis, subsequently merging. Patches of complete RBC hemolysis appeared after 100 min drying time, which leads to the formation of the outer semi-impermeable protective barrier as drying time increased. Indeed, no RBC was detected at the surface of the spheroid after 120 min of drying time. The thickness of this thin protective film was characterized as a function of blood volume. Thickness of the surface barrier increased as the volume of spheroid increased where an average film thickness of 0.91, 4.7, 12.8, and 15.5 µm were measured for 4, 10, 25, and 50 µL dried blood spheroids,

respectively. Drying times for these spheroids were kept at a comparable 4 h period (Figure S9). Larger blood volumes wet the hydrophobic paper to a greater extent due to larger mass, which causes surface tension forces of the droplet to be overcome by blood-paper surface interactions. These spheroids have a greater number of RBC interactions and are subject to a greater degree of environmental stressors (e.g., exposure to aerobic oxidation) which predisposes the RBCs at the blood-air interface to a faster rate of hemolysis. Not surprisingly, the thickness of the protective layer increases with storage/drying time as observed for a 10 µL dried blood spheroid, which showed 4.7 µm protective barrier after 4 h drying period compared with 30 µm film thickness after 504 h (21 days) of storage.

Based on these experimental data, we can summarize the mechanism of formation of dried blood spheroids as follows (Figure 4): First, solvent evaporation occurs at the blood-air interface, generating capillary flow[38] that transports blood proteins (e.g., fibrinogen) and red blood cells towards the outer peripheral of the blood drop. The fibrinogens confer high coagulative abilities to the region of proteins/RBCs at the peripheral, which undergoes a sol-gel transition. As solvent continues to evaporate, RBCs begin to self-assemble and form stacks of rouleau, a process which ceases at approximately 60 min (Figure 4B). These surface RBCs are no longer protected by hydration shells and are subject to oxidative stress and were observed to lose their disk-like conformation after approximately 80 min due to hemolysis. This period marks the onset of RBC destruction/lysis under the dried blood spheroid storage condition (Figure 4C), which exhibits a hemolysis suppression factor of at least 8X when compared with the conventional DBS method where only a few RBCs are detected after 10 min of blood collection.

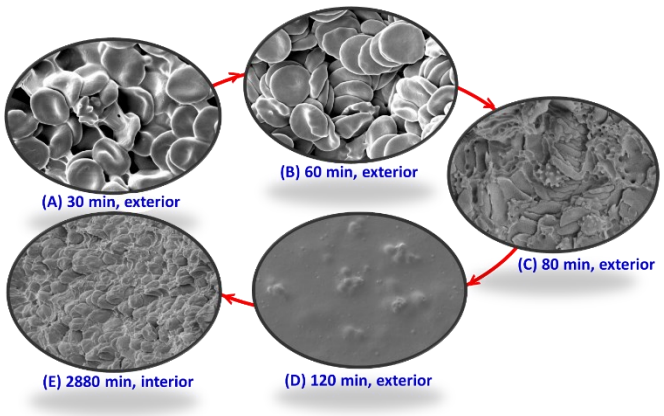

Figure 4. Sequence of red blood cell (RBC) assembly and deformation during the creation and storage of dried blood spheroids on hydrophobic paper substrate. (A) Within <30 min of drying the spheroids, solvent evaporation results in the bridging between individual RBCs, which marks the onset of their self-assembly process. (B) The peak of the RBC self-assembly process occurs at 60 min drying time for 10 µL blood drop where the RBCs aggregate to form the stable rouleau conformation. (C) Hemolysis of RBC at the spheroid's surface leads to the deformation of the rouleau conformation, which commences at 80 min of drying time. (D) By 120 min in the spheroid's drying process, all RBCs at the surface of the spheroid lyse due to excessive hemolysis, which leads to the formation of the passivation layer at exterior of dried blood spheroid. (E) Although no RBCs are detected at exterior of the spheroid at 120 min, intact red cells are still detected at the interior bulk of dried blood spheroid even after 2880 min storage under ambient conditions.

Interestingly, hemolysis is a well-controlled process under the spheroid storage condition that begins at the surface of the dried blood. The localized nature of the process and the rate at which the RBCs located in the interior of the spheroid lyse led to the proposition that the first lysed layer of the RBCs at the surface of the spheroid serves to passivate the interior of the spheroid. Complete formation of the surface protective layer is not observed until 120 min of drying time (Figure 4D). As discussed above, the thickness of this layer gradually increases, progressing deeper into the core of the spheroid as more RBCs undergo hemolysis. Figure 4E shows the interior of dried blood spheroid after 2880 min (48 h) of formation, revealing intact RBCs in their native disk-like shape and showing no signs of hemolysis despite the blood sample being stored at room temperature.

The presence of anticoagulant ethylenediaminetetraacetic acid (EDTA) is likely influencing the rate of formation of the protective barrier which leads to differences in resulting barrier thickness. To investigate the impact of anticoagulant on the formation of this passivation layer, a comparative study was performed on whole blood obtained from a K2-EDTA-capped tube and from a finger stick. Whole blood (10 µL) from each sample set was deposited onto hydrophobic paper substrate and were air-dried under ambient conditions for 2 h. The samples were then subject to SEM sample fixation (Figure S10). Blood obtained from a finger stick had a protective barrier of 112 µm compared to a protective barrier of 11 µm from a similarly prepared sample obtained from the K2-EDTA-capped tube. These results suggest that anticoagulants affect the rate at which the protective barrier forms (e.g., due to the reduction in RBC interactions during the solvent evaporation stage). The resulting barrier thickness is greater in samples without anticoagulant present because a greater number of RBCs interact with clotting factors, thus facilitating coagulation via bridging and subsequent hemolysis.

It is important to note that the hemolysis of surface RBCs occurs at the blood-air interface as well as at the paper-blood interfaces. It has been shown that the drying of blood on hydrophobic surfaces begins at the triple line where blood, surface, and air meet.[39] As such, we observed the peripheral edges of the spheroid to dry first, leading to higher concentrations of fibrinogen at the paper-blood interface due to the rapid water evaporation in this area. Coagulation of blood on a hydrophobic interface is also well-known, which can lead to fibrin formation.[40] In our study, fibrin located at the paper-blood interface was observed to be anchored in the empty pores of the paper once the blood is fully dried (Figure S11). It is also possible that the tiny fibers at the surface of the rough porous hydrophobic paper might be embedded in the blood. These phenomena (i.e., fibrin formation and protruding paper fibers) provides a strong anchoring mechanism for the dried

blood spheroid that firmly secures the blood sample to the surface of the paper substrate.

Physical Characterization of Dried Plasma and Serum

Plasma and serum samples were prepared on hydrophobic and hydrophilic paper substrates and subsequently characterized by SEM after fixation with 2.5% glutaraldehyde in 0.1 M phosphate buffer (pH 7.4) for a minimum of 72 hours. Dried plasma and serum samples conformed to 3D hemisphere-like structures on hydrophobic paper while drying as 2D spots on hydrophilic paper (Figure S1-S4). For the same biofluid volume (10 µL), whole blood formed the most spherical structure, with the largest height (defined as the distance from the approximate center of the biofluid from the biofluid-paper substrate interface to the apex of the biofilm, the biofluid-air interface) measuring 896 µm from the base of the paper. Biofilms from plasma and serum exhibited heights of 390 and 350 µm, respectively (Figure S12). The differences in the heights of the 3D structures derived from the three biofilms can be ascribed to the presence or absence of biomacromolecules. Whole blood contains RBCs, which are much larger than other proteinaceous components found in plasma or serum. The resulting dried blood can maintain a spherical structure due to the high viscosity and strong self-assembly of red blood cells. Plasma and serum do not contain RBCs and therefore are less viscous. Although plasma and serum have similar structures when dried, a slight difference stems from the presence of clotting proteins/factors in plasma compared to serum, which lacks such clotting proteins/factors.

Chemical Characterization of Biofilms: Stabilization of Cocaine in Dried Plasma and Serum Samples using Hydrophobic Paper

One well known advantage of dry-state biofluid samples is the low shipment requirement. A major application of microsampling that commonly requires shipment of dry-state samples is in pharmacokinetics. However, this experiment often employs plasma samples as opposed to whole blood. Unfortunately, the use of DBS in pharmacokinetics is limited because it is not straightforward to compare data obtained from DBS to that from plasma due to complications associated with the level of blood cells. For this reason, DPS have been proposed as an alternative for DBS to create opportunities to use dry-state samples in drug development programs, which tend to favor plasma as the preferred matrix. Such a platform can be utilized in clinical trials for samples generated across the globe (including resource-limited settings) to facilitate effective sample sharing between different analytical laboratories.

Plasma and serum samples are relatively viscous although lacking RBCs. We hypothesized that dry-state plasma and serum samples can be stabilized at room temperature when prepared on hydrophobic paper due to self-assembly of larger biomacromolecules forming a protective shell. Note that DPS and DSS are conventionally prepared using hydrophilic paper substrates. We used cocaine in this study since previous studies demonstrated it to be labile when stored in dry state at room temperature.[20,30] We spiked 2 µg/mL of cocaine in whole blood, plasma, and serum, and 4 µL aliquots were deposited separately onto hydrophobic and hydrophilic paper triangles. All samples were air-dried and subsequently analyzed via paper spray MS in MS/MS mode (cocaine *m/z* 304 → 182) using cocaine-d3 (*m/z* 307 → 185) as the internal standard. We monitored the cocaine signal relative to that of the internal standard over a period of 15 days and normalized the data using the A/IS signal from fresh samples (i.e., day 0). The results from these experiments are summarized in Figure 5, where a stable cocaine signal was obtained for all samples prepared on hydrophobic paper. On the contrary, the signal for cocaine in DBS, DPS, and DSS samples prepared on hydrophilic paper degraded quickly (within two days) upon drying at room temperature. When comparing the stability of cocaine in all three biofilms, cocaine degraded more quickly in plasma and whole blood (day 1) than in serum (day 2). This could be due to interruptions in protein-binding interactions with cocaine.

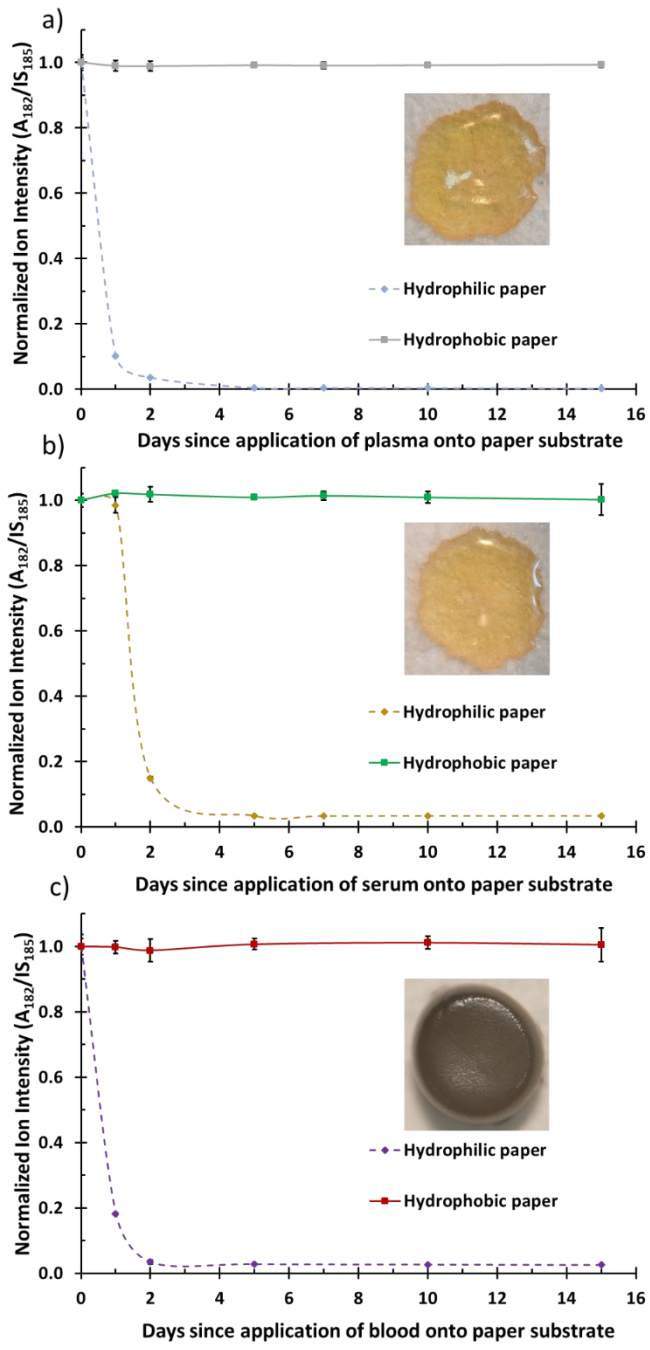

Figure 5. Stability of cocaine in (A) dried plasma, (B) dried serum, and (C) dried blood spheroid on hydrophilic paper and hydrophobic paper substrates. Cocaine-d3 was used as internal standard (IS). The ratio of analyte (A) signal (transition, *m/z* 304 → 182) to IS (transition, *m/z* 307 → 185) signal (A/IS) was monitored for 15 days and was normalized to A/IS derived from day zero (0). The inset depicts dried plasma, serum, and whole blood 3D morphologies (top-down) on hydrophobic paper substrate.

As shown in the insets, when applied on hydrophobic paper, whole blood, plasma, and serum forms a 3D scaffold which serves to protect the interior bulk. Like dried blood spheroids, a protective barrier forms in plasma and serum which serves to stabilize the interior bulk of the 3D dried matrix. The 3D structure is completely absent when deposited on hydrophilic paper and thus exposing the entire sample to oxidative stress which degrades the labile cocaine analyte.

Conclusions

In summary, microsampling through the adsorption process of biofluids on hydrophobic paper substrates is observed to present a more favorable room temperature dry-state storage condition than the conventional dried blood spot method that is based on an absorption mechanism. The protective mechanism for dried blood spheroids is revealed in this work to involve the formation of a surface barrier made of lysed red blood cells. The semi-impenetrable nature of the surface film is ascribed to the initial formation of tightly packed stacks of red blood cells observed in the form of rouleau conformation. The rouleau form because of solvent evaporation at the blood-air interface, which concentrates large biomolecules (e.g., fibrinogen) to act as bridging entities between individual red cells. This bridging mechanism in 3D blood spheroids on hydrophobic paper is observed experimentally for the first time. The red blood cells at the surface are subsequently subjected to oxidative stress and merge to form a thin barrier that protects the interior of the dried blood spheroid. These mechanistic insights were obtained from high resolution data garnered from scanning electron microscopy experiments.

The general protective power of 3D surface films was tested by storing plasma and serum on hydrophobic paper, which showed enhanced stability for cocaine, a property that is likely due to self-assembly of large biomolecules such as clotting factors. The ability to enhance analyte stability in untreated biofluids on inexpensive paper substrates at room temperature is essential for biomarker discovery and disease diagnosis in resource-limited settings. For example, light microscopy, the current gold standard for malaria diagnosis, cannot be used for the analysis of dried blood prepared by the traditional dried blood spot method due to rapid hemolysis. The ability to preserve red blood cells in the dry state on hydrophobic paper might open doors for the screening of remotely collected dried blood samples for malaria diagnosis by reconstituting the samples and analyzing them. Direct mass spectrometry analysis of the stored biofluid is also possible through paper spray ionization, which is found to be more effective when using hydrophobic paper substrates. 3D biofilms on hydrophobic paper utilizes an adsorption mechanism of sample deposition which reduces sample-paper interactions, thus enhancing extraction processes and subsequently sensitivity.

Electronic Supplementary Information (ESI)

Experimental details are provided in the Electronic Supplemental Information that includes hydrophobic paper preparation, paper spray conditions, MS parameters, procedure

for spheroid fixation in glutaraldehyde solution, SEM parameters and additional discussion on physical changes in red blood cell morphology.

Conflicts of interest

There are no conflicts to declare.

Acknowledgements

This research was supported by National Institute of Health (Grant Number R01-AI-143809) and National Science Foundation (Award Number CHE-1900271). Electron microscopy was performed at the Center for Electron Microscopy and Analysis (CEMAS) at The Ohio State University and the Campus Microscopy & Imaging Facility (CMIF) at The Ohio State University.

Notes and references

1 P. H. J. Riegman, M. M. Morente, F. Betsou, P. de Blasio and P. Geary, *Molecular Oncology*, 2008, **2**, 213–222.
2 P. H. J. Riegman, W. N. M. Dinjens and J. W. Oosterhuis, *Pathobiology*, 2007, **74**, 239–244.
3 S. Chen, Q. Wan and A. K. Badu-Tawiah, *Journal of the American Chemical Society*, 2016, **138**, 6356–6359.
4 S. Korenev, H. Lemonde, M. Cleary and A. Chakrapani, *Paediatrics and Child Health*, 2019, **29**, 105–110.
5 P. Denniff and N. Spooner, *Anal. Chem.*, 2014, **86**, 8489–8495.
6 C. L. Bowen, H. Licea-Perez, M. Z. Karlinsey, K. Jurusik, E. Pierre, J. Siple, J. Kenney, A. Stokes, N. Spooner and C. A. Evans, *Bioanalysis*, 2013, **5**, 1131–1135.
7 B. S. Frey, D. E. Damon and A. K. Badu-Tawiah, *Mass Spec Rev*, 2019, 1–35.
8 D. Blessborn, K. Sköld, D. Zeeberg, K. Kaewkhao, O. Sköld and M. Ahnoff, *Bioanalysis*, 2013, **5**, 31–39.
9 I. I. Slowing, C.-W. Wu, J. L. Vivero-Escoto and V. S.-Y. Lin, *Small*, 2009, **5**, 57–62.
10 I. Medina Diaz, A. Nocon, D. H. Mehnert, J. Fredebohm, F. Diehl and F. Holtrup, *PLoS ONE*, 2016, **11**, 1–18.
11 A. Y. Chan, R. Swaminathan and C. S. Cockram, *Clinical Chemistry*, 1989, **35**, 315–317.
12 F. Al-Khafaji, A. Bowron, A. P. Day, J. Scott and D. Stansbie, *Annals of Clinical Biochemistry: An international journal of biochemistry and laboratory medicine*, 1998, **35**, 780–782.
13 J. A. Kluge, A. B. Li, B. T. Kahn, D. S. Michaud, F. G. Omenetto and D. L. Kaplan, *Proc Natl Acad Sci USA*, 2016, **113**, 5892–5897.
14 P. M. Edelbroek, J. van der Heijden and L. M. L. Stolk, *Therapeutic Drug Monitoring*, 2009, **31**, 327–336.
15 R. C. Knudsen, W. E. Slazyk, J. Y. Richmond and W. H. Hannon, *Guidelines for the Shipment of Dried Blood Spot Specimens*, Centers for Disease Control and Prevention, 1995.
16 A. Sharma, S. Jaiswal, M. Shukla and J. Lal, *Drug Test. Analysis*, 2014, 399–414.
17 P. W. Smit, I. Elliott, R. W. Peeling, D. Mabey and P. N. Newton, *The American Journal of Tropical Medicine and Hygiene*, 2014, **90**, 195–210.
18 A. F. Olshan, *Environmental Health Perspectives*, 2007, **115**, 1767–1779.
19 D. A. Lacher, L. E. Berman, T.-C. Chen and K. S. Porter, *Clinica Chimica Acta*, 2013, **422**, 54–58.
20 D. E. Damon, M. Yin, D. M. Allen, Y. S. Maher, C. J. Tanny, S. Oyola-Reynoso, B. L. Smith, S. Maher, M. M. Thuo and A. K. Badu-Tawiah, *Anal. Chem.*, 2018, **90**, 9353–9358.
21 E. L. Rossini, D. S. Kulyk, E. Ansu-Gyeabourh, T. Sahraeian, H. R. Pezza and A. K. Badu-Tawiah, 16.
22 D. E. Damon, K. M. Davis, C. R. Moreira, P. Capone, R. Cruttenden and A. K. Badu-Tawiah, *Anal. Chem.*, 2016, **88**, 1878–1884.
23 E. van der Linden and E. Allen Foegeding, in *Modern Biopolymer Science: Bridging the Divide between Fundamental Treatise and Industrial Application*, Elsevier/Academic Press, Amsterdam Boston, 2009, pp. 29–91.
24 T. Yakhno, *Journal of Colloid and Interface Science*, 2008, **318**, 225–230.
25 A. K. Martusevich, Y. Zimin and A. Bochkareva, *Hepatitis Monthly*, 6.
26 Y. Zheng, X. Zhang, H. Yang, X. Liu, X. Zhang, Q. Wang and Z. Zhang, *Anal. Methods*, 2015, **7**, 5381–5386.
27 X. Wang, Y. Zheng, T. Wang, X. Xiong, X. Fang and Z. Zhang, *Anal. Methods*, 2016, **8**, 8004–8014.
28 F. Han, Y. Yang, J. Ouyang and N. Na, *Analyst*, 2015, **140**, 710–715.
29 Z. Zhang, W. Xu, N. E. Manicke, R. G. Cooks and Z. Ouyang, *Analytical Chemistry*, 2012, **84**, 931–938.
30 D. J. Swiner, S. Jackson, G. R. Durisek, B. K. Walsh, Y. Kouatli and A. K. Badu-Tawiah, *Analytica Chimica Acta*, 2019, **1082**, 98–105.
31 P. Basuri, A. Baidya and T. Pradeep, *Anal. Chem.*, 2019, **91**, 7118–7124.
32 J. W. Field, *Transactions of the Royal Society of Tropical Medicine and Hygiene*, 1949, **43**, 33–48.
33 P. G. Shute and M. Maryon, *Transactions of the Royal Society of Tropical Medicine and Hygiene*, 1960, **54**, 415–418.
34 O. K. Baskurt and H. J. Meiselman, *Microcirculation*, 2008, **15**, 585–590.
35 O. K. Baskurt, B. Neu and H. J. Meiselman, *Red Blood Cell Aggregation*, Taylor & Francis Group, 2011.
36 C. Wagner, P. Steffen and S. Svetina, *Comptes Rendus Physique*, 2013, **14**, 459–469.
37 S. Asakura and F. Oosawa, *J. Polym. Sci.*, 1958, **33**, 183–192.
38 K. Sefiane, *Advances in Colloid and Interface Science*, 2014, **206**, 372–381.
39 B. Sobac and D. Brutin, *Colloids and Surfaces A: Physicochemical and Engineering Aspects*, 2014, **448**, 34–44.
40 L.-C. Xu, J. W. Bauer and C. A. Siedlecki, *Colloids and Surfaces B: Biointerfaces*, 2014, **124**, 49–68.

